MANTECH Publications

Journal of Computer Aided Manufacturing and Automation
Volume 4, Issue 1, January-June, 2019

Stress Analysis of a Thick Walled Orthotropic Bonded Cylinder under Pressure and Temperature by Using FEM

Somnath Somadder[1], Md. Shahidul Islam[2]

Department of Mechanical Engineering

Khulna University of Engineering & Technology, Khulna, Bangladesh

***Corresponding Authors' email id**: somnathsomadder@yahoo.com[1], shahidulbitk@gmail.com[2]*

Abstract

The behavior of material subjected to thermo mechanical loads is of interest to researchers in a wide variety of discipline. Axi symmetric pressure vessels have wide use in industrial engineering. They often operate under combined mechanical and thermal loads which may be constant or cycling. The combined effects of temperature and pressure must be taken into account when designing cylinders. Cylinders have wide application in chemical, petroleum and military industry. Various methods of prestressing techniques such as compound cylinder, increasing wall thickness are used so that thick cylinders can resist large internal pressure and to make effective use of material at the upper portion of the cylinder. In this thesis work the analytical and numerical analysis of compound thick cylinder is given. The evaluation of the resistance and the conformity of the cylinders depending upon the conditions of use are illustrated by stress and displacement distributions. The results of the analytical approach are validated to a finite element model.

Keywords: *Stress analysis, Prestressing, Compound cylinders, Analytical and finite element analysis*

INTRODUCTION

The design of thick walled cylinders for operation at very high temperatures and pressure is a complex problem involving various considerations including definition of the operating and permissible stress levels, criteria of failure, material behavior etc. Generally problems involving

cylinders have been widely used due to their practical importance. In order to improve the safety and reliability of cylinder under various thermo-mechanical loads it is really important for engineers to optimize the design.

Over the last decade, finite element analysis (FEA) stopped being regarded only as an analyst's tool and entered the practical world of design engineering. CAD software now comes with built-in FEA capabilities and design engineers use FEA as an everyday design tool in support of the product design process. However, until recently, most FEA applications undertaken by design engineers were limited to linear analysis. Such linear analysis provides an acceptable approximation of real-life characteristics for most problems design engineers encounter. Nevertheless, rarely more challenging problems arise, problems that call for a nonlinear approach. Non-linear behavior of solids takes two forms: material non-linearity and geometric non-linearity. The simplest form of non-linear material behavior is that of elasticity for which the stress is not linearly proportional to the strain. More general situations are those in which the loading and unloading response of the material is different. Typical here is the case of classical elastic– plastic behavior.

Thick walled cylinders are broadly used in chemical, petroleum, military industries as well as in nuclear power plants. They are usually subjected to high pressure & temperatures which may be constant or cycling. Industrial problems often witness ductile fracture of materials due to some discontinuity in geometry or material properties. The conventional elastic analysis of thick walled cylinders to final radial & hoop stresses is applicable for the internal pressure up to yield strength of material. General application of Thick-Walled cylinders include, high pressure reactor vessels used in metallurgical operations, process plants, air compressor units, pneumatic reservoirs, hydraulic tanks, storage for gases like butane LPG etc. [1].

Interfaces between reinforcement and matrix in composite materials; metal and ceramic in electronic packaging and metal coating; ceramic and polymer in biomaterials; sensor and structural components in smart structures; and solder joints in electronics are some of the typical examples of bi-material interface.. Strength of bi-material joint greatly depends on the orientation of physical

properties and material structure. If the physical properties of any material are symmetric about an axis that is normal to a plane of isotropy then it is called transversely isotropic material. This transverse plane has infinite planes of symmetry and thus, within this plane, the material properties are the same in all directions. The theory of transversely isotropic elastic materials is an important branch of applied mathematics and engineering science. With the rapid development of modern technology, the theory of transversely isotropic elasticity has become increasingly important. Bi-material joint is also sensitive to the changes in the geometrical parameters. These geometrical parameters affect the performances of a bonded joint. It is well known that there are discontinuities of material and geometry at the bonding edges in these joints. These discontinuities may cause singularities in the stress fields or very stress concentration near the vertex of the bonding edges. This stress concentration/singularity may lead to the delamination initiation in the local area, and subsequently to the global failure of the joint structures (Hu et al.1998; De Chen and Chue, 2003). That is why most researches on bi- material interfaces deal with the stress singularity. To characterize the interface properties, sound knowledge on the stress singularity is required [2].

Previously many analysis have done in the literature of the cylinders. Several research studies have been conducted and reported to determine permissible stress levels, criteria of failure and material behavior at the interface of bi metallic cylinder.

Zhang et al. [3] derived an analytical solution to determine of the thermo-mechanical stresses of a multilayered compound pressure vessel considering the influence of closed ends. Vedeld et al. [4] derived analytical expressions for the displacement field and corresponding stress state in two-layer cylinders subjected to mechanical and thermal loading. Sollund et al. [5] developed analytical recursive algorithms for calculating stresses and displacements in heated, pressurized, multi-layer cylinders in plane stress or plane strain conditions. The use of composite materials have widely been investigated. An overview of advanced materials was provided by David et al. [6] for hydrogen storage. Design of bimetallic cylinder was investigated by Wilson et al. [7]. Moreover transient response of hollow cylinder with hybrid boundary conditions was also determined [8-10]. Xu& Yu [11] carried down

shakedown analysis of internally pressurized thick walled cylinders, with material strength differences. Through elasto-plastic analysis, the solutions for loading stresses, residual stresses, elastic limit, plastic limit & shakedown limit of cylinder are derived. M. Imanijed& G. Subhash [12] developed a universal solution for plastic deformation of thick-walled cylinders subjected to internal pressure and proportional loading. Elastic-plastic behavior is also investigated numerically by Poworznek [13]. Kautor [14] investigated displacement field and stress of a compound cylinder subjected to pressure and temperature. Minimization of material volume of multilayer cylinders subjected to pressure load was investigated by Patil [15]. Bursting pressure analysis was determined by Hareram [16]. In elastic and plastic range stress variation was also analyzed by Tajana[17].

In this paper, the resulting stress and displacement fields in orthotropic compound cylinders subjected to thermo-mechanical loads are presented. The analytical solutions are compared with finite element solutions.

MATHEMATICAL MODELING

In the present study, a thermo-elastic model is introduced to describe the behavior of compound cylinders subjected to internal pressure with the presence of a temperature change between the inner and outer wall of the assembly. First of all temperature distribution is determined considering conduction heat transfer through the various side surfaces of the cylinders in the radial direction. Then using the stress-strain relations the equilibrium equation for a cylinder with axial symmetry and the strain-displacement relationship, the resulting stresses and displacements from the application of internal pressure are calculated in order to determine the optimum working conditions of the cylinder.

For the assembly used in this study, T_1 is the fluid temperature in contact with the inside wall of the inner cylinder, T_2 is the temperature of the contact surface between the two cylinders and T_3 is the ambient temperature at the outer surface of the outer cylinder. Here, a, b and c are the compound cylinder radius.

In the steady state, the heat flux, Q is conserved across the different layers of the cylinders and it can be written for compound cylinder

$$Q = \frac{2\pi K_1 L}{\ln\left(\frac{b}{a}\right)}(T_1 - T_2) = \frac{2\pi K_2 L}{\ln\left(\frac{c}{b}\right)}(T_2 - T_3) \quad (1)$$

Where, $K_{1,2}$ is the thermal conductivity of cylinder 1 and 2 respectively and L is the length of the two cylinders. Since the problem is axisymmetric, the temperature distribution depends only on radial position r.

Hence, the temperature distribution for the cylinder $C_{yi}(i = 1, 2)$

$$T_{cyi}(r) = (T_{in} - T_{out})\left(\frac{\ln\left(\frac{r_{out}}{r}\right)}{\ln\left(\frac{r_{out}}{r_{in}}\right)}\right) + T_{out} \quad (2)$$

Now from above expressions considering one of the two cylinders $C_{yi=1,2}$ subjected to the radial temperature variation T_{cyi} the stress strain relationship can be written according to Ref. [18],

$$\begin{aligned}
\sigma_r^{\,i} &= \frac{E_i}{(1+\nu_i)(1-2\nu_i)}\left[(1-\nu_i)\varepsilon_r^{\,i} + \nu_i\varepsilon_\theta^{\,i} - (1+\nu_i)\alpha_i T_{cyi}\right] \\
\sigma_\theta^{\,i} &= \frac{E_i}{(1+\nu_i)(1-2\nu_i)}\left[(1-\nu_i)\varepsilon_\theta^{\,i} + \nu_i\varepsilon_r^{\,i} - (1+\nu_i)\alpha_i T_{cyi}\right] \\
\sigma_z^{\,i} &= \nu_i\left(\sigma_r^{\,i} + \sigma_\theta^{\,i}\right) - E_i\alpha_i T_{cyi}
\end{aligned} \quad (3)$$

The equilibrium equation for cylinder with axial symmetry is given by [18]:

$$\frac{d\sigma_r}{dr} + \frac{\sigma_r^{\,i} - \sigma_\theta^{\,i}}{r} = 0 \quad (4)$$

The strain displacement relationship for the long cylinder is written as,

$$\varepsilon_r^i = \frac{du_i}{dr}; \varepsilon_\theta^i = \frac{u_i}{r}; \varepsilon_z^i = 0 \quad (5)$$

From equation (3) and equation (5)

$$\frac{d}{dr}\left[\frac{1}{r}\frac{du_i}{dr}\right] = \frac{(1+\nu_i)}{(1-\nu_i)}\alpha_i\frac{dT_{cyi}}{dr} \quad (6)$$

Integrating equation (6),

$$u_i(r) = \frac{(1+\nu_i)}{(1-\nu_i)}\left(\frac{\alpha_i}{r}\right)\int_{r_{in}}^{r}\rho T_{cyi}d\rho + C_{i1}r + \frac{C_{i2}}{r} \quad (7)$$

Where C_{i1} and C_{i2} are the constants of integration for cylinder $C_{yi=1,2}$

Using the displacement given by equation (7) and stress strain relationship by equation (5), the radial and hoop stress becomes,

$$\begin{aligned}
\sigma_r^{\,i} &= E_i\left[-\frac{\alpha_i}{(1-\nu_i)r^2}\int_{rin}^{r}\rho T_{cyi}d\rho + \frac{C_{i1}}{(1+\nu_i)(1-2\nu_i)} - \frac{C_{i2}}{(1+\nu_i)r^2}\right] \\
\sigma_\theta^{\,i} &= E_i\left[\frac{\alpha_i}{(1-\nu_i)r^2}\int_{rin}^{r}\rho T_{cyi}d\rho + \frac{C_{i1}}{(1+\nu_i)(1-2\nu_i)} + \frac{C_{i2}}{(1+\nu_i)r^2} - \frac{\alpha_i T_{cyi}}{(1+\nu_i)}\right]
\end{aligned} \quad (8)$$

The integration constants, C_{ij} are determined using the boundary conditions in the compound cylinders. These boundary conditions are related to the application of the internal pressure, pi, the

continuity of the radial displacement and the radial stress at the interface layer between the two cylinders. They are summarized in the following equation:

$$\sigma_r^{\,1}(a) = -p_i ; \sigma_r^{\,2}(c) = 0$$
$$\sigma_r^{\,1}(b) = \sigma_r^{\,2}(b) ; u_1(b) = u_2(b) \quad (9)$$

Substituting the temperature distributions, stresses and displacements of the inner and outer Cylinders into the boundary conditions, the equations system, given by Eq. (19), is obtained

$$\begin{bmatrix} 1 & k_{12} & -1 & -k_2 \\ 1 & k_{22} & k_{23} & k_{24} \\ 1 & k_{32} & 0 & 0 \\ 0 & 0 & 1 & k_{44} \end{bmatrix} \begin{bmatrix} C_{11} \\ C_{21} \\ C_{12} \\ C_{22} \end{bmatrix} = \begin{bmatrix} B_1 \\ B_2 \\ B_3 \\ B_4 \end{bmatrix} \quad (10)$$

With:

$$k_{22} = -\frac{(1-2\nu_1)}{b^2} = \frac{a^2}{b^2} k_{32} = \frac{c^2}{b^2} k_{44}$$

$$k_{12} = -k_{14} = \frac{1}{b^2}$$

$$k_{23} = -\left(\frac{E_2}{E_1}\right)\left(\frac{1+\nu_1}{1+\nu_2}\right)\left(\frac{1-2\nu_1}{1-2\nu_2}\right) = -k_{24}\left(\frac{b^2}{(1-2\nu_2)}\right)$$

$$B_1 = \left(\frac{1+\nu_1}{1-\nu_1}\right)\left(\frac{\alpha_1}{b^2}\right)\int_a^b \rho T_{cyi} d\rho = -B_2 \frac{1}{1-2\nu_1}$$

$$B_3 = \frac{(1-2\nu_1)(1+\nu_1)}{E_1} p_i$$

$$B_4 = \alpha_2 \left(\frac{1+\nu_2}{1-\nu_2}\right)\left(\frac{1-2\nu_2}{c^2}\right)\int_b^c \rho T_{cy2} d\rho$$

By obtaining the integration constant we can calculate the stress and displacements at each radial position from equation (7) and (8).

FINITE ELEMENT MODEL

The validation of the proposed analytical model is done by using finite element model with ABAQUS software. Simulation was done by considering the cylinder subjected to thermo-mechanical loads. As this is a thermo-mechanical analysis mesh element type is usedC3D8T which is an 8-node thermally coupled brick, trilinear displacement and temperature.

To examine the material properties effect on the behavior of the cylinder steel is used for single cylinder and for compound cylinder steel and aluminum is used. Loads are changed to observe the effect of loads on the stress and displacement fields. For inner cylinder carbon epoxy is used and for outer cylinder graphite epoxy is used for the analysis. Coupled temperature displacement is usually performed by first conducting an uncoupled heat transfer analysis and then a stress analysis.

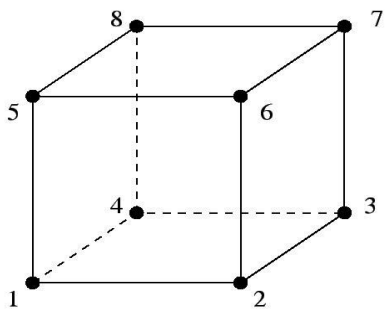

Fig. 1: 8 node brick element

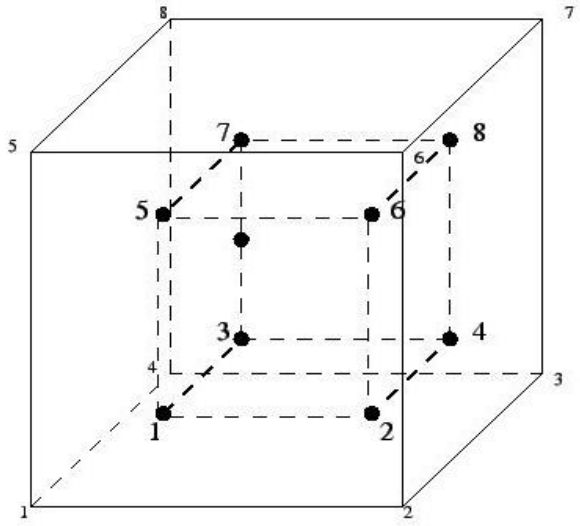

Fig. 2: 2x2x2 integration point scheme in hexahedral elements

The C3D8T element is a general purpose linear brick element, fully integrated (2x2x2 integration points).

PHYSICAL ASPECTS OF THE MODEL

In this analysis two cylindrical element have chosen to analyze. The inner cylinder having inner radius, a = 0.01 m and outer radius b = 0.02m. The outer cylinder having inner radius b = 0.02 m and outer radius c = 0.03 m. The inner cylinder is made of carbon epoxy and outer cylinder is made of graphite epoxy. Bimetallic interface occurs at r = b = 0.02 m. Length of the cylinder z = 0.05 m.

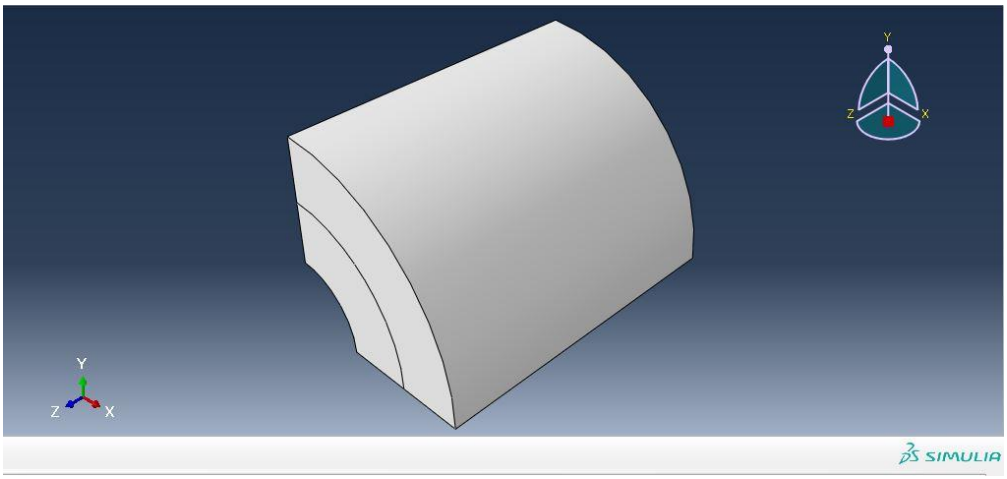

Fig. 3: Isometric view of the cylinder for analysis

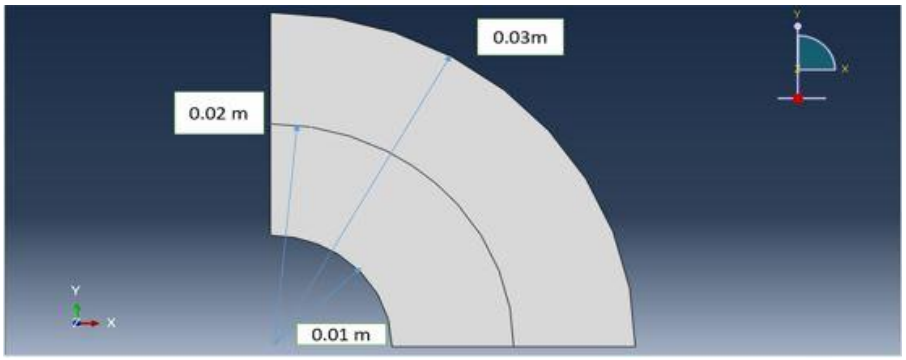

Fig. 4 Model for analysis in XY plane

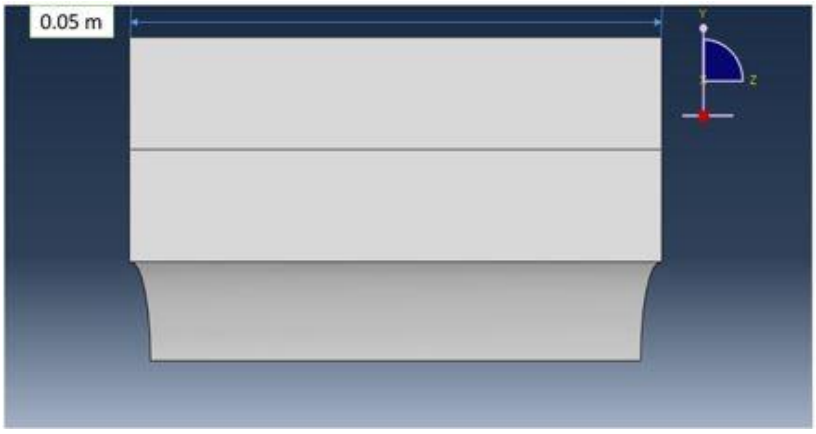

Fig. 5: Model for analysis in YZ plane

Whenever fluid passes through a cylinder it exerts a certain amount of pressure P_i= *1 MPa*, if the fluid is hot then heat transfer will occur by heat conduction process. T_{in}=*160*℃, T_{out}=*25*℃.

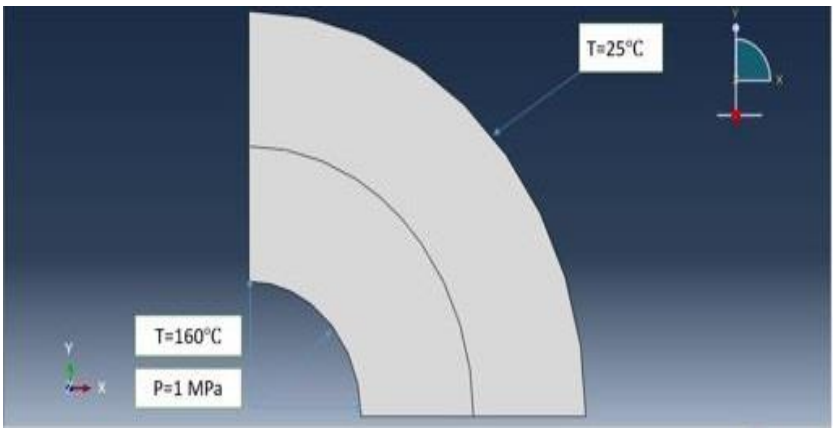

Fig. 6: Model showing the boundary conditions

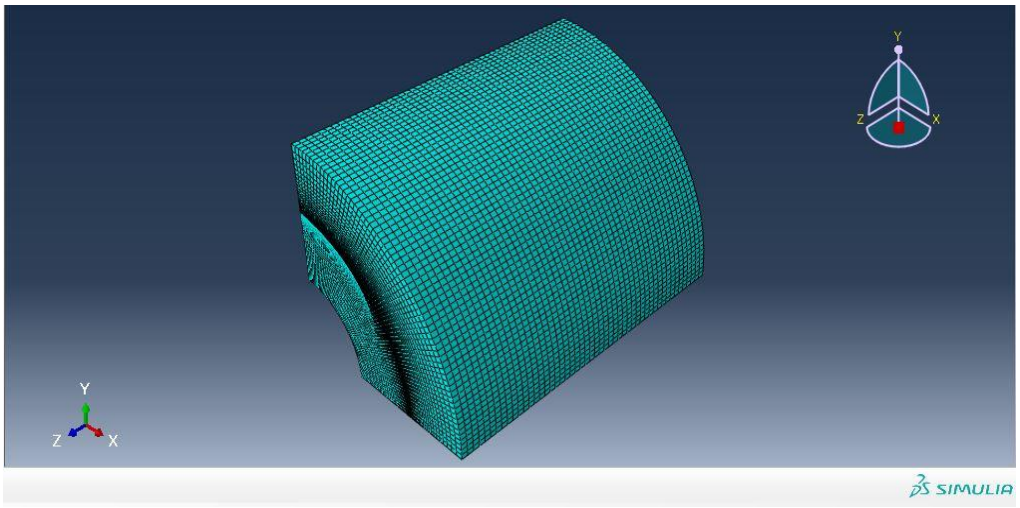

Fig.7:. Mesh picture of the model.

Table 1: Mechanical properties of orthotropic materials []

Material	$E_1(GPa)$	$E_2(GPa)$	$E_3(GPa)$	ν_{12}	ν_{23}	ν_{13}	G_{12} (GPa)	G_{23} (GPa)	G_{13} (GPa)
Carbon epoxy	147	10.3	10.3	.27	.54	.27	7	3.7	3.7
Graphite epoxy	131	10.342	10.342	.33	.22	.49	6.8	6.2	6.2

Since at the interface material property changes so bias has been used so there is more element near the interface than the inner and outer side of the cylinder. As this is a thermo-mechanical analysis mesh element type is usedC3D8T which is an 8-node thermally coupled brick, trilinear displacement and temperature.

MATERIAL PROPERTIES

Material carbon epoxy and graphite epoxy is used as orthotropic material. Here carbon epoxy is used as lower material and graphite epoxy as upper material. The mechanical properties of carbon epoxy and graphite epoxy are shown in table 1.

Material orientation

(a)

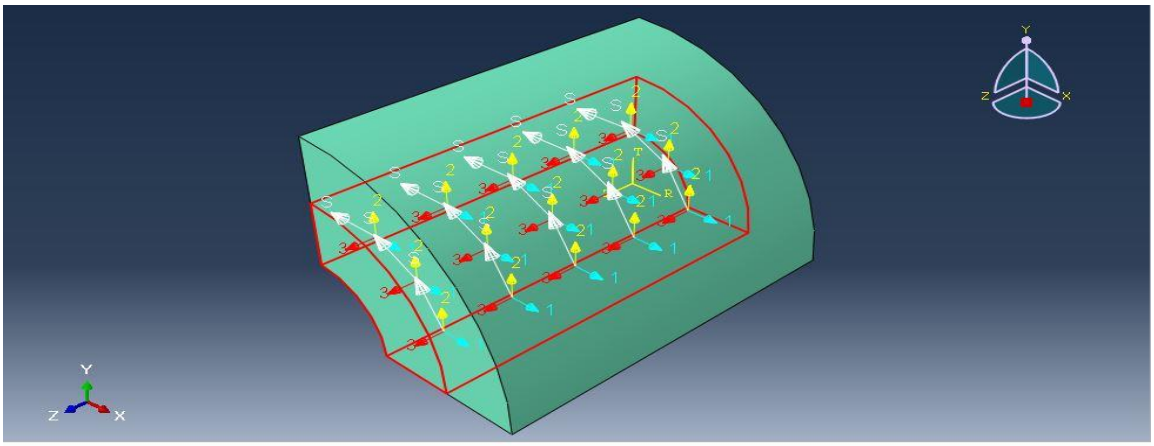

(b)

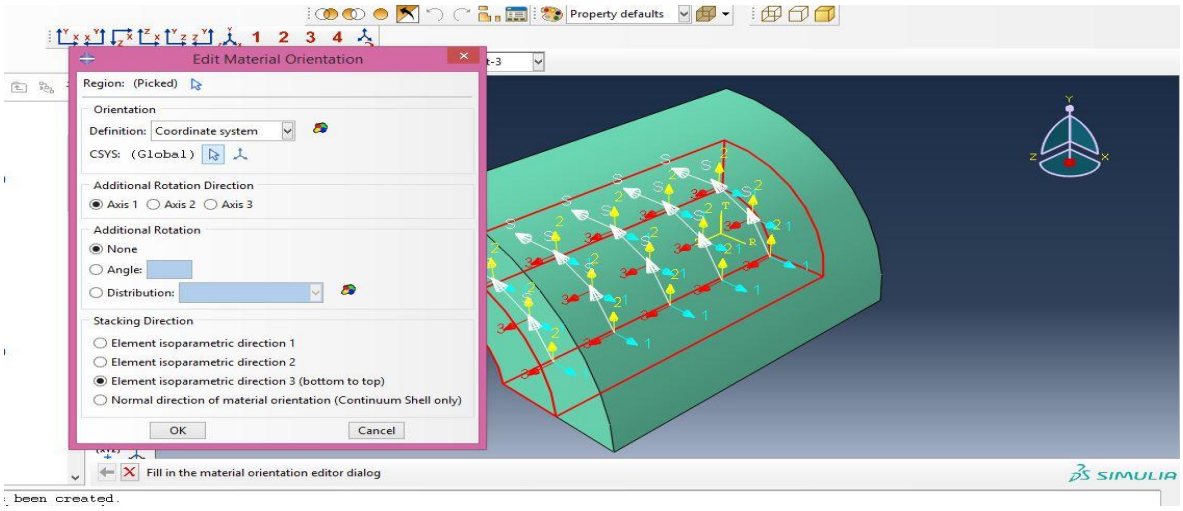

Fig.8: (a) Material orientation of the lower part of the cylinder (b) how orientation was created.

A coordinate system is defined to create the orientation of the lower part of the cylinder additional rotation is also fixed.

(a)

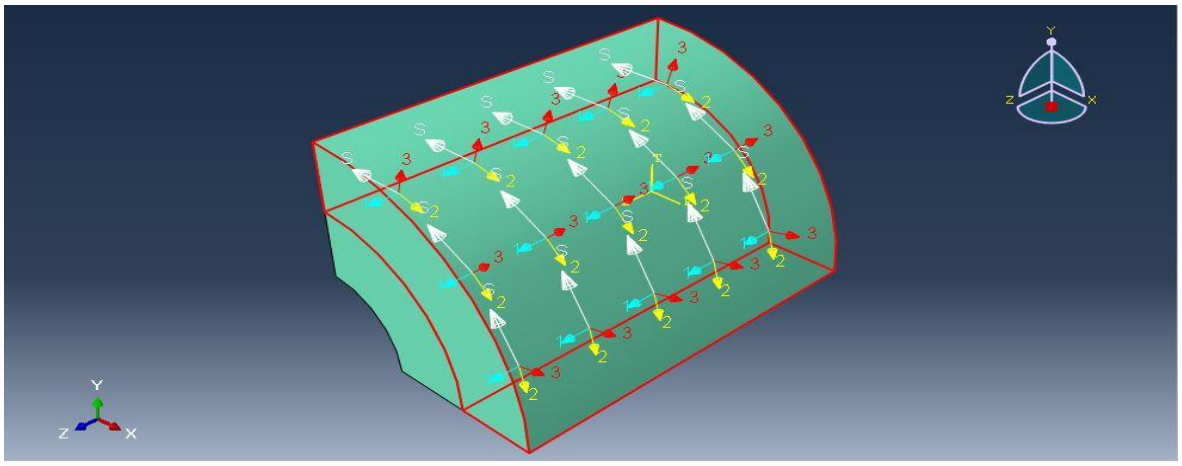

(b)

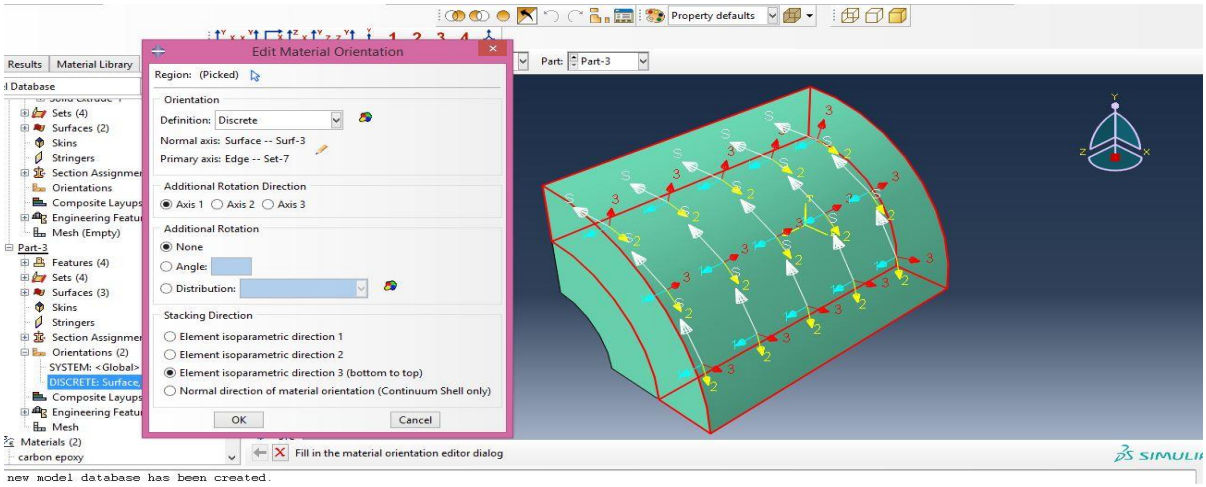

Fig.9: (a) Material orientation of the upper part of the cylinder (b) how orientation was created.

A discrete system is defined to create the orientation of the upper part of the cylinder additional rotation is also fixed.

ACCURACY VERIFICATION

In this work two published papers were verified. Firstly analysis of Susanta Chowdhury [2] and Kauotor Bahoum [17] was analyzed by using ABAQUS software then the accuracy was determined by using Plot Digitizer software. By using Plot Digitizer software we can extract data's from any published research paper and compare our data with that data's. It was observed that error of my data's are less than 1%. The comparison of the results are illustrated in figure 10 and 11.

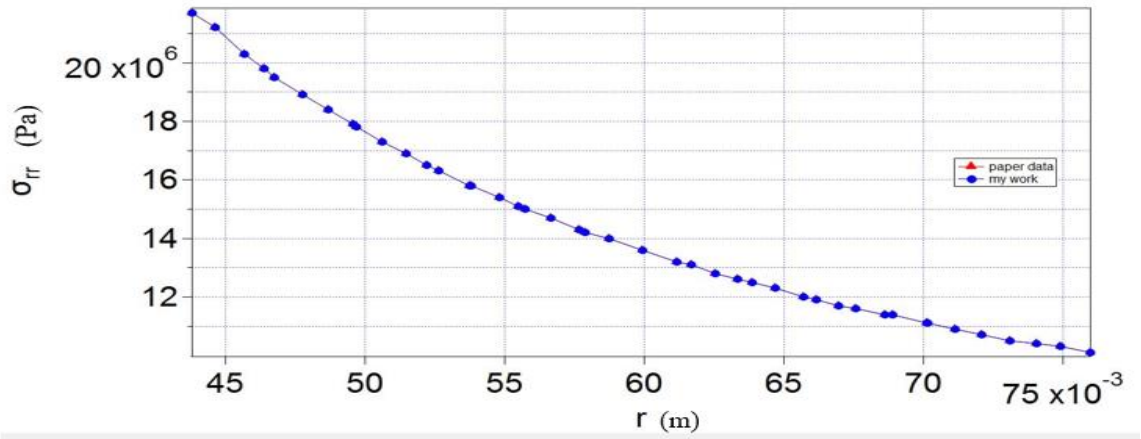

Fig.10: Comparison of my work and Susanta Chowdhury's research for determining variation of radial stress along radius subjected to internal pressure.

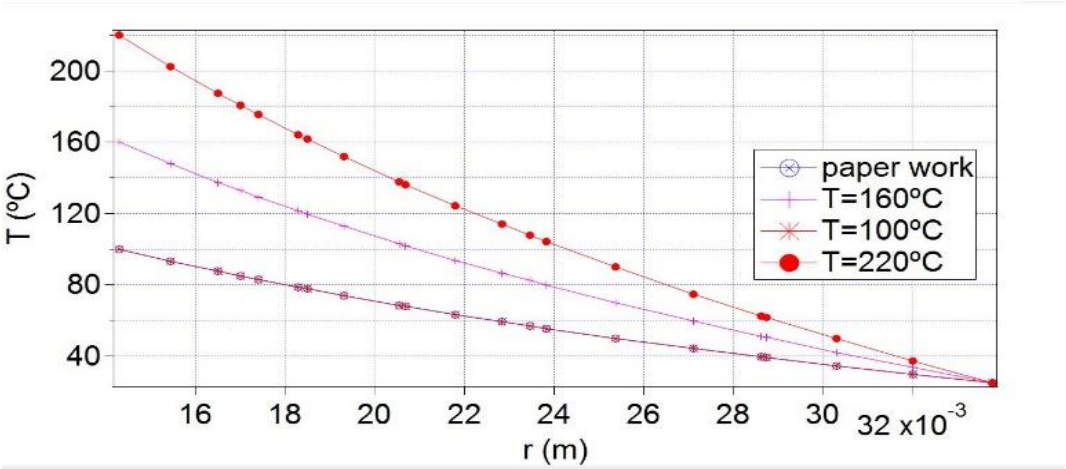

Fig.11: Comparison of my work and Kauotor Bahoum's research for determining temperature variation along radius of compound cylinder.

MESH SENSITIVITY ANALYSIS:

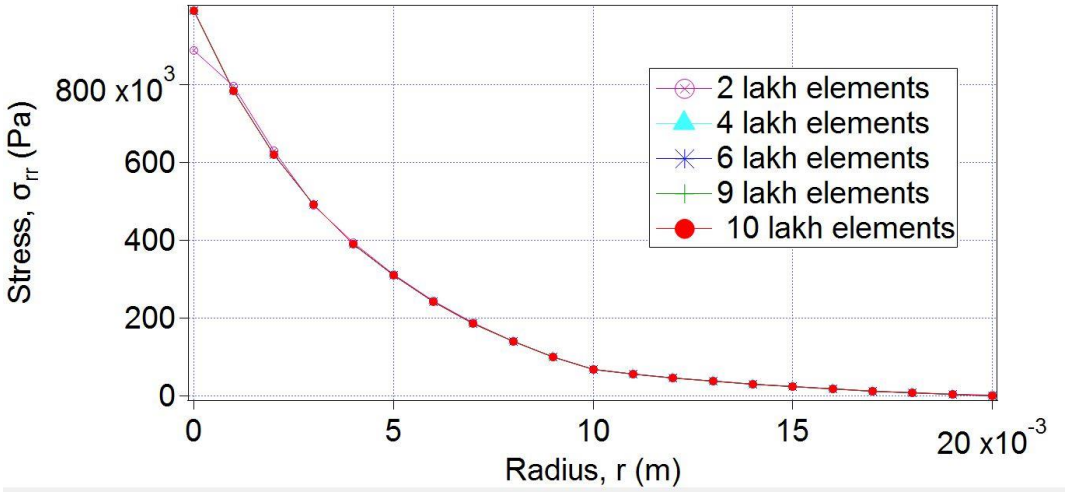

Fig. 12: Mesh sensitivity analysis of the work showing variation of radial stress along the true distance of the radius.

In case of numerical analysis mesh sensitivity analysis is the most important issue. The main objective of numerical analysis is to obtain the most accurate result in the shortest possible time. Here different mesh size and different number of elements was imposed on the model to verify the accuracy of work.

From the figure it is clear that results are not so accurate using 2 lakh elements. Accuracy of the result is increased as element number is increased from 2 lakh to 10 lakhs. It was observed that the results obtained using 9 lakh elements is same as the result obtained 10 lakh elements.

So, there is no reason to use 10 lakh elements and increase the computational time. So the optimum number of elements is found 9 lakh. Further analysis was done using this optimum number of elements.

RESULT AND DISCUSSION

In this present work, ABAQUS software was used to analyze the stress and displacement variation of a thick walled cylinder under pressure and temperature. Firstly the model was analyzed under pressure and then the model was analyzed under combined pressure and temperature loading.

The estimation of the resistance and the compliance of the compound cylinders,

depending upon the condition of use are explained by the stress and displacement distributions through various layer thickness. Here, FEM is used for finding approximate solutions of differential equations in physical problems under boundary conditions.

Approximate solutions are formed in each element and then assembled to main equation. Iterative process is maintained in computing each and every nodal data. Finally, the unknown results are calculated using the main FEM equation. Symmetric boundary conditions are used as the geometry is symmetric and the boundary conditions are also symmetric. So, quarter of the model is used for analysis, resulting in fewer degrees of freedom and computational costs. The graphical presentations and the contours are shown below.

This graph indicates that there is no discontinuity at the interface r = .02 m for components and the boundary condition is satisfied. Sharp change occurs for inside cylinder material and stress variation is not so large in case of outside cylinder material.

Using pressure load only:

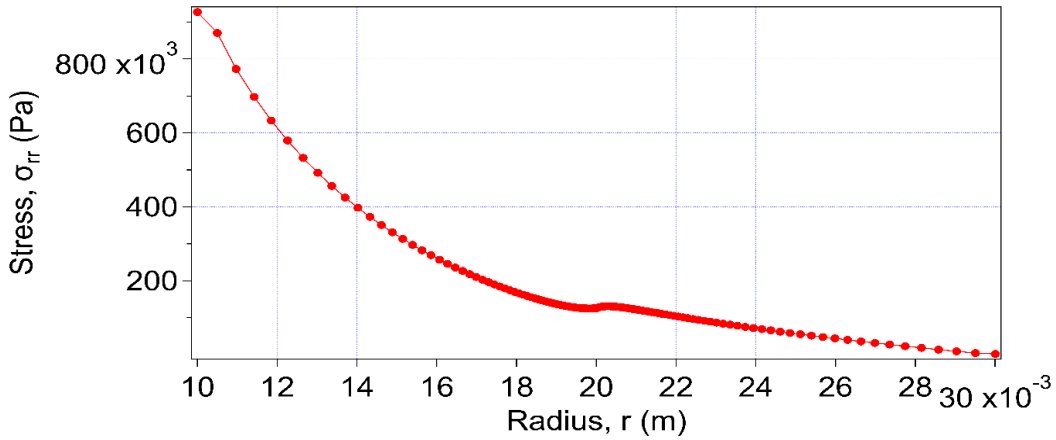

Fig. 13: Variation of stress σ_{rr} components along radius at $\theta = 90°$

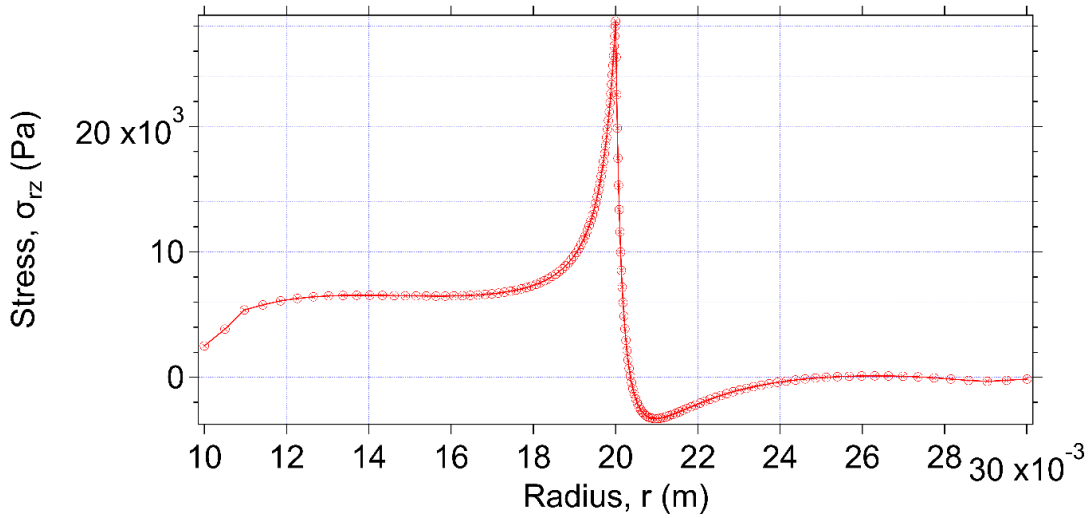

Fig. 14: Variation of stress σ_{rz} components along radius at $\theta = 90°$.

This graph indicates that there is no discontinuity at the interface r = 0.02 m for components and the boundary condition is satisfied. The stress is maximum at the interface region and the change in the stress for inside material increases with radial distance but stress in outside material decreases with radial distance. There is sharp change of stress distribution for both of inside and outside cylinder materials.

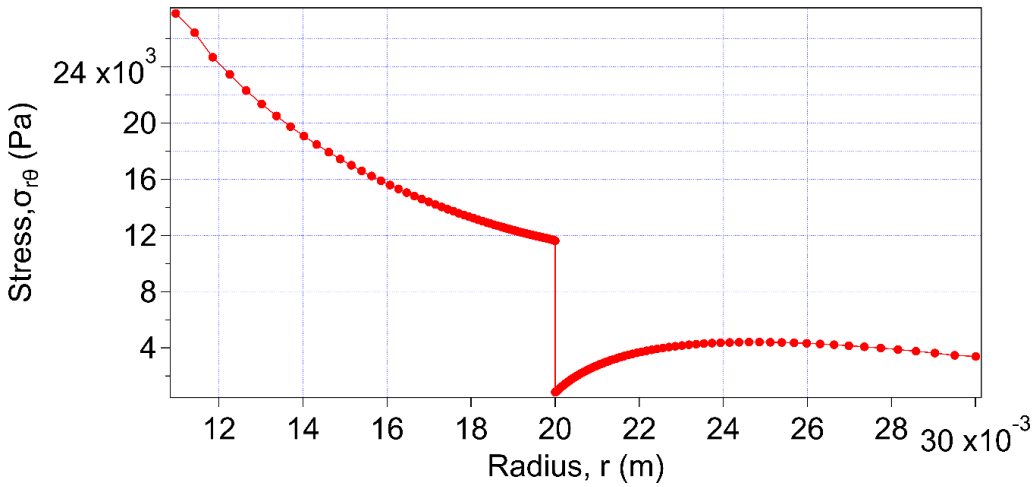

Fig.15: Variation of stress $\sigma_{r\theta}$ components along radius at $\theta = 90°$.

It is clear that there is jump at the interface r = 0.02 m. So, the boundary condition is not satisfied. This may occur due to the mismatch material properties, loads applied on the model is excessive that the joint may break here.

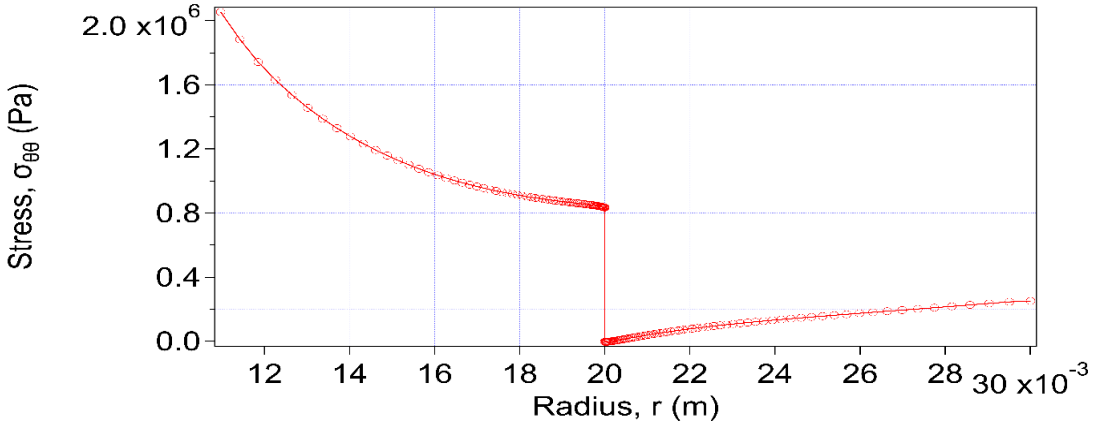

Fig. 16: Variation of stress $\sigma_{\theta\theta}$ components along radius at $\theta = 90°$.

From figure it is clear that there is jump at the interface r = 0.02 m. So, the boundary condition is not satisfied. Variation in the inside cylinder is more smooth than for the material of the outside cylinder. Firstly stress decreases from maximum to the interface for inside material and for outside material stress increases with the radial distance from the interface. These discontinuities can occur due to the irregularities of orthotropic materials.

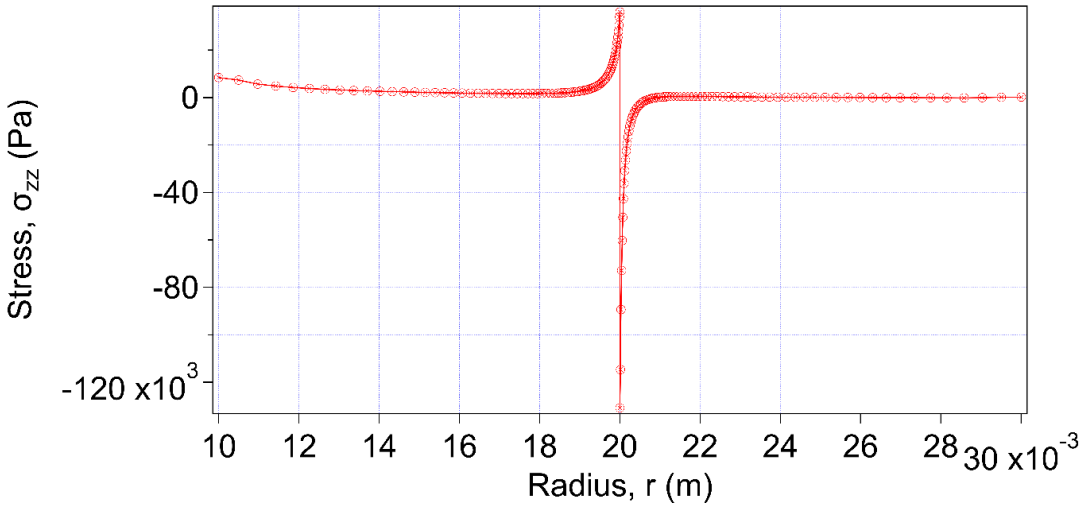

Fig. 17: Variation of stress σ_{zz} components along radius at $\theta = 90°$.

This graphs indicates that there is discontinuity at the interface for components and the boundary condition is not satisfied. As the materials are orthotropic it may cause irregularity in the stress distribution. Mismatch of the material properties can provide this type of result. Firstly the stress for the inside cylinder material decreases, then increases at the interface region with increase of radius up to the contact point. A jump occurs at the interface. For the outside cylinder the stress also increases with radial distance.

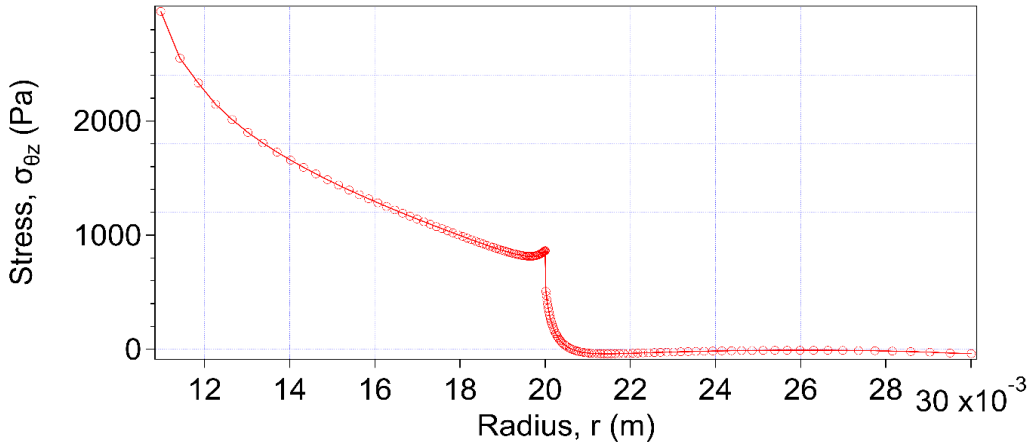

Fig. 18: Variation of stress $\sigma_{\theta z}$ components along radius at $\theta = 90°$.

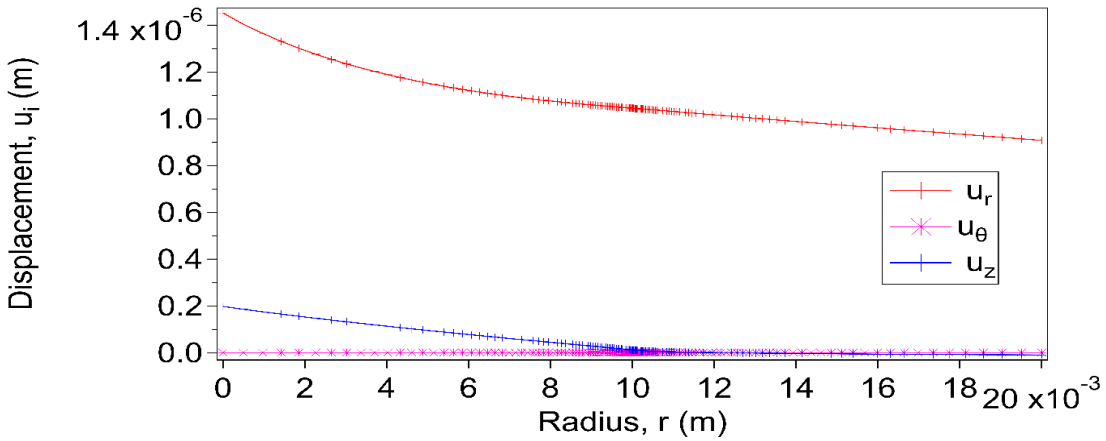

Fig. 19: Variation of displacement components along the radius at $\theta = 90°$.

The graph shows the variation of stress component in tangential face and z direction with the change of radial distance. Firstly for the inside cylinder the stress decreases sharply up to the interface then at the interface there is a slight jump.

After that stress for the outside cylinder material initially decreases rapidly near the interface then after certain distance the change of stress is very small. This discontinuity may be removed by further meshing the model. **See Figure 18**

It is clear that at the contact radius there is no discontinuity of displacement variation and the boundary condition is satisfied. Here, u_θ shows very small amount of displacement compare to u_r and u_z. Displacement components u_r and u_z are asymmetric in nature. Boundary conditions are satisfied at the interface as there is no jump in the contact point. A sharp change of displacement occurs for the material of the inside cylinder and the displacement change is small for the material of the second cylinder.

8.2 Using pressure and temperature load

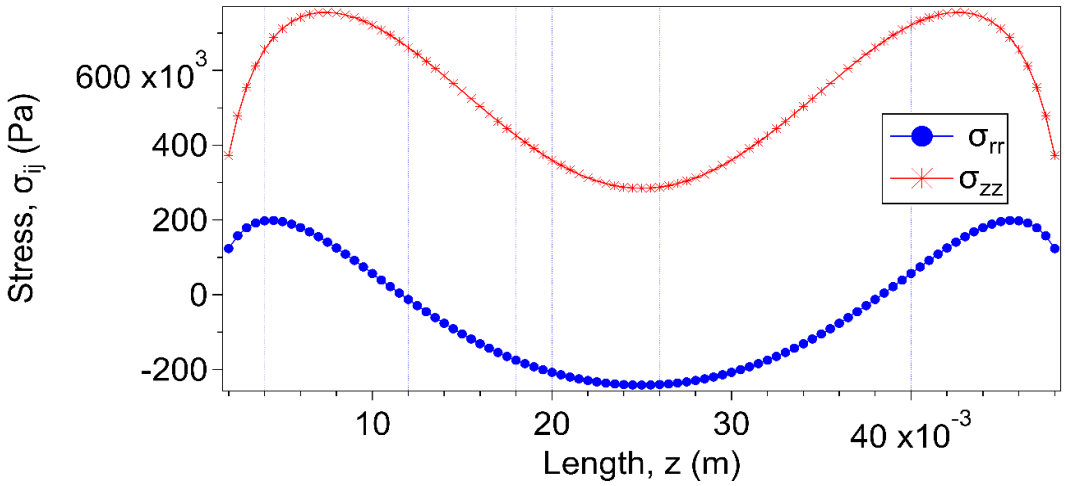

Fig.20: Variation of σ_{rr} and σ_{rz} along the length of the cylinder $\theta = 90°$.

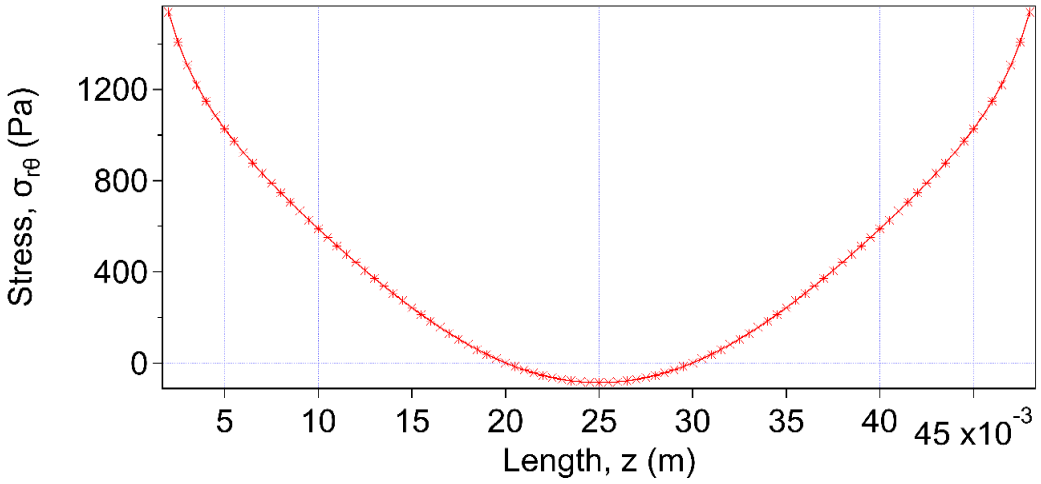

Fig. 21: Variation of $\sigma_{r\theta}$ along the length of the cylinder $\theta = 90°$.

In figure 20-21 the variation of stress components at the interface along the length is shown. There is a large change near the middle region of the cylinder. Stress component has maximum value at the free edge vertex of the joint. Normal stresses components and symmetric about z = 0.025 m.

The shear stress is also symmetric in r face and direction. For above three cases stress continues to decrease up to z = 0.025 m with increase of distance from the vertex and then increases after z= 0.025m with increase of distance towards vertex of the joint.

In this figure the stress component σ_{rz} variation is antisymmetric about $z = 0.025m$. This may occur due to the irregularity in the material properties of the orthotropic cylinder. As the distance increases from the free edge vertex stress decreases up to zero at z = 0.025 m and after z= 0.025m stress is also decreased as distance is increased to another vertex of the joint.

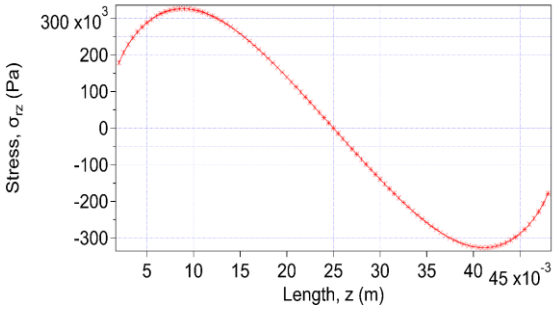

Fig. 22: Variation of σ_{rz} along the length of the cylinder $\theta = 90°$.

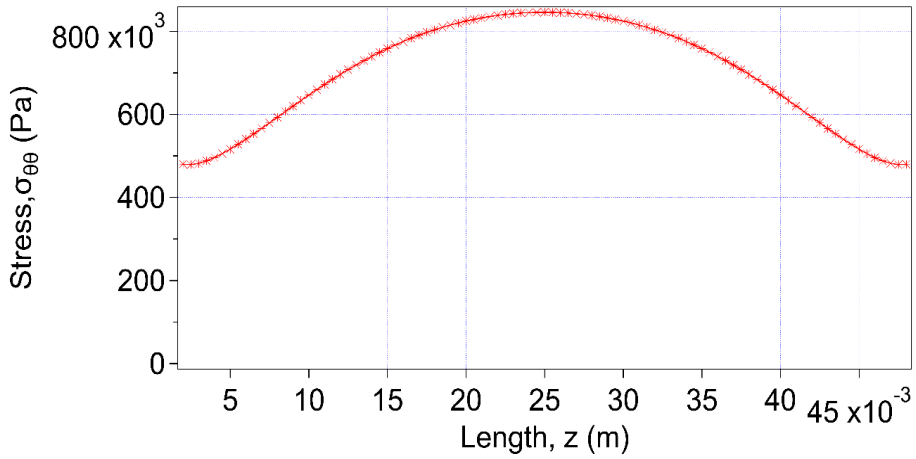

Fig. 23: Variation of $\sigma_{\theta\theta}$ along the length of the cylinder $\theta = 90°$.

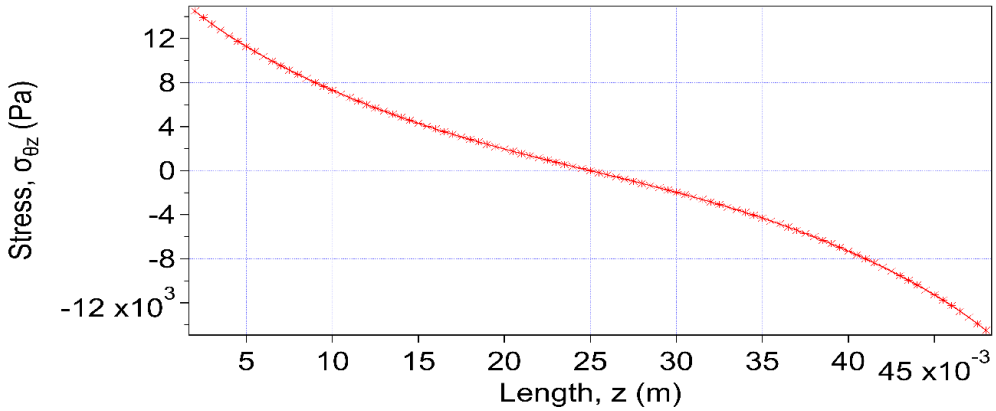

Fig. 24: Variation of $\sigma_{\theta z}$ along the length of the cylinder $\theta = 90°$.

In this figure the stress component variation $\sigma_{\theta\theta}$ is symmetric about $z = 0.025m$. Firstly stress component increases with distance up to z = 0.025 m and then it starts to decrease up to free edge of the vertex of the joint. There is smooth distribution of stress components throughout the distance. No noise or discontinuity is observed along the joint. See Figure 23

In this figure the stress component variation $\sigma_{\theta z}$ is antisymmetric about $z = 0.025m$. This may occur due to the irregularity in the material properties of the orthotropic cylinder. Firstly stress decreases with increase of distance and reaches to zero at z = 0.025 m. After that stress continues to decrease further with increase of distance as it approaches vertex of the joint.

Figure 25 indicates the variation of displacement components along length. Displacement components in radial is symmetric near the middle range and displacement in the tangential direction is constant along the length. u_θ shows small displacement compared to displacement component in the r and z directions. Displacement components in the r direction is maximum near the vertex of the joint. Displacement component in the z direction is asymmetric in nature where displacement reduces up to zero as distance increase up to z=0.025m then a sharp decrease in displacement component occur with increase of distance.

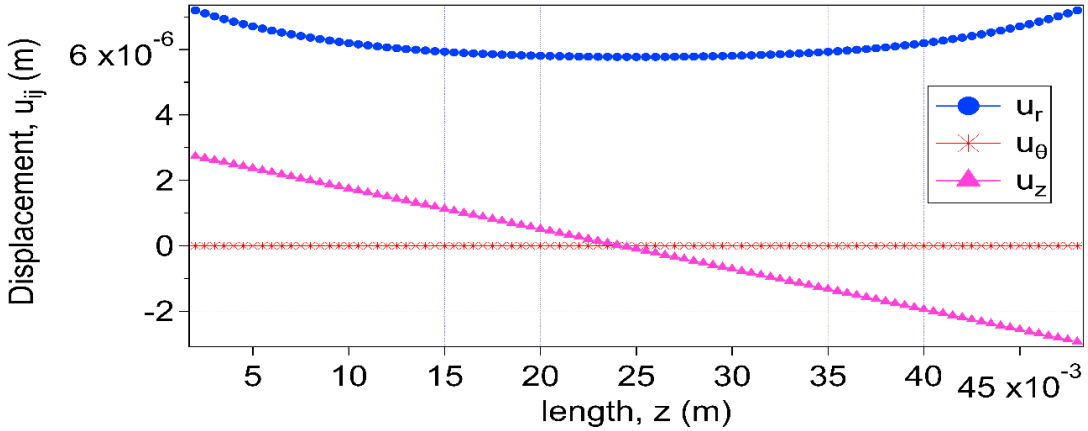

Fig. 25: Variation of u_{ij} along the length of the cylinder $\theta = 90°$.

4.5 Surface plots of the stress and displacement component

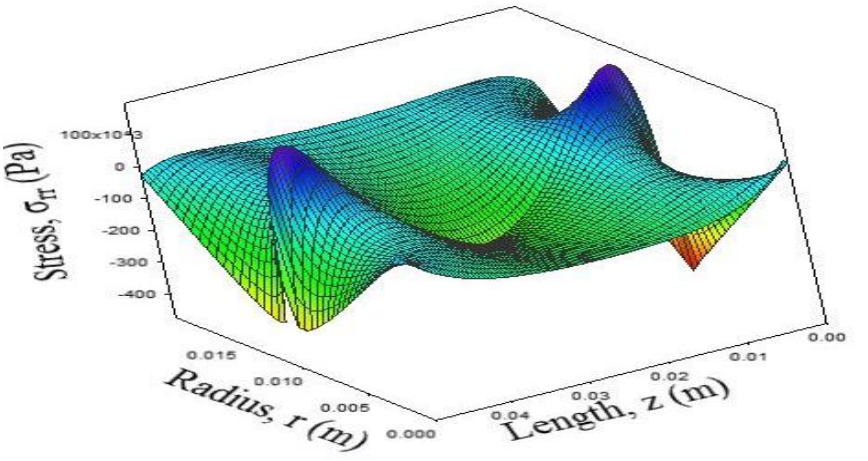

Fig. 26: Variation of stress component σ_{rr}

Maximum stress occur at the interface region r = 0.01 m. So extra material should be added at the interface to prevent debonding. Stress component has maximum value at the free edge vertex of the joint. Normal stresses components and symmetric about z = 0.025 m.

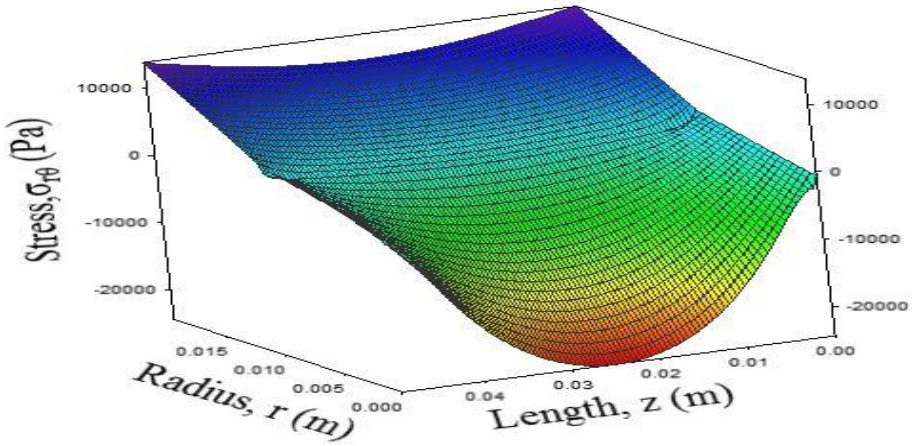

Fig. 27: Variation of stress component $\sigma_{r\theta}$

From this surface plot it is clear that stress varies sharply for the material of the inside cylinder and slight change in stress distribution occurs for the outside cylinder. Nature of the 2D and 3D surface plot is also same.

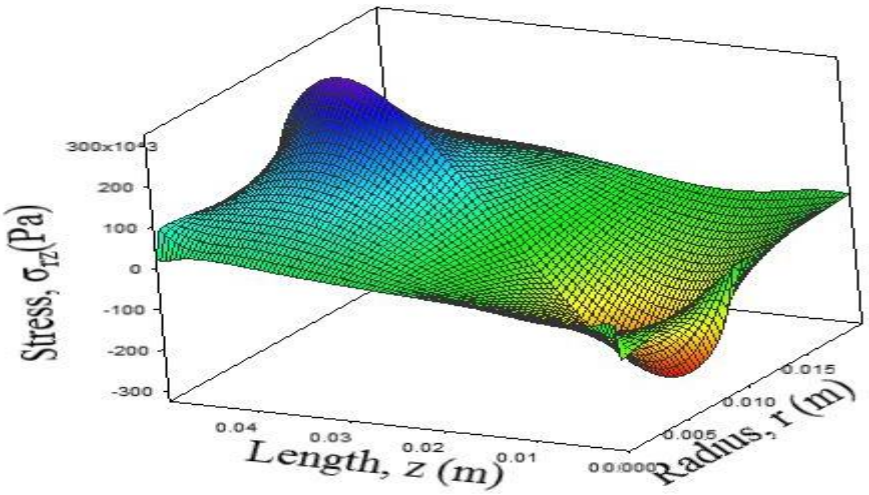

Fig. 28: Variation of stress component σ_{rz}

σ_{rz} variation is antisymmetric about $z = 0.025m$. This may occur due to the irregularity in the material properties of the orthotropic cylinder. Variation of stress component is sharp for the inside cylinder rather than the outside cylinder. As the distance increases from the free edge vertex stress increases up to zero at *z = 0.025 m* and after *z = 0.025 m* stress is also increased as distance is increased to another vertex of the joint.

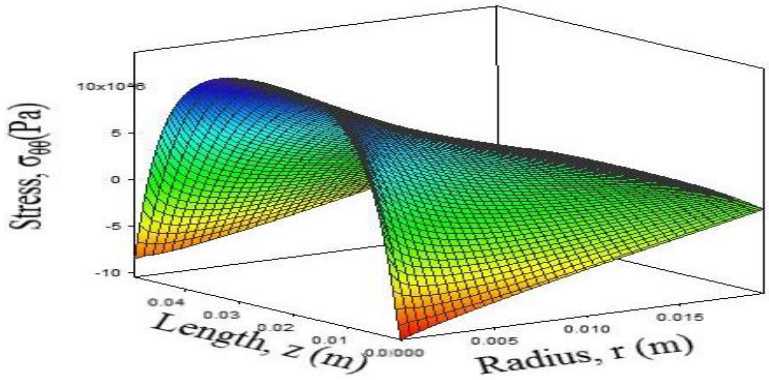

Fig. 29: Variation of stress component $\sigma_{\theta\theta}$

The stress component variation $\sigma_{\theta\theta}$ is symmetric about $z = 0.025m$. Firstly stress component increases with distance up to z = 0.025 m and then it starts to decrease up to free edge of the vertex of the joint. There is smooth distribution of stress components throughout the distance. No noise or discontinuity is observed along the joint.

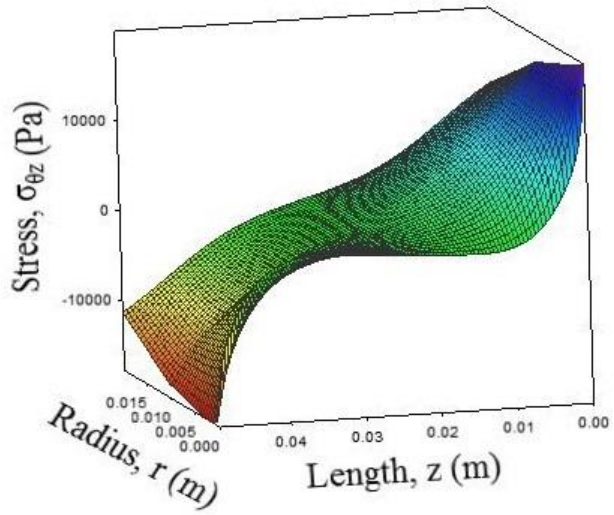

Fig. 30: Variation of stress component $\sigma_{\theta z}$

The stress component variation $\sigma_{\theta z}$ is antisymmetric about $z = 0.025m$ .Stress variation is quite same in nature for inside and outside cylinder. Firstly stress decreases with increase of distance and reaches to zero at z = 0.025 m. After that stress continues to decrease further with increase of distance as it approaches vertex of the joint.

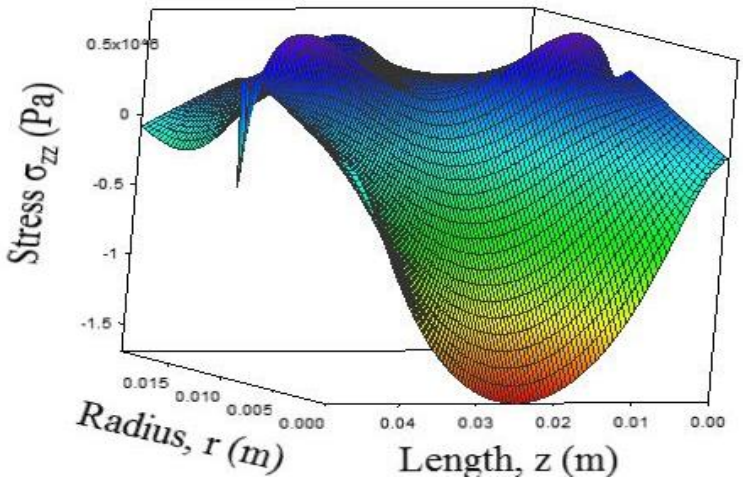

Fig. 31: Variation of stress component σ_{zz}

Figure 31 indicates variation of various stress components. In these curves there are no discontinuities at the interface. Normalized stress components in z plane and z direction is symmetric. Nature of the 2D curves and 3D surface plots are similar.

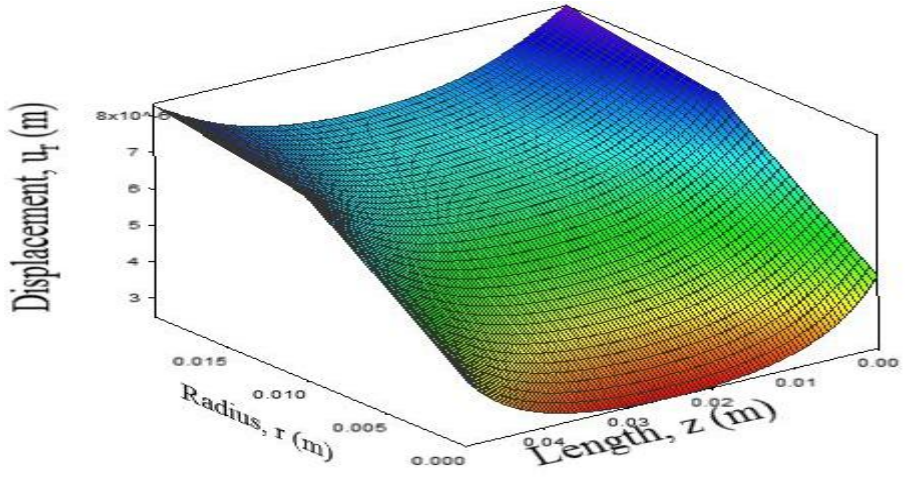

Fig. 32: Distribution of displacement components u_r

A drastic change of displacement components along radius is noticed for the inside cylinder. Smooth distribution of displacements throughout the interface as there is no noise in the curve and jump at the interface.

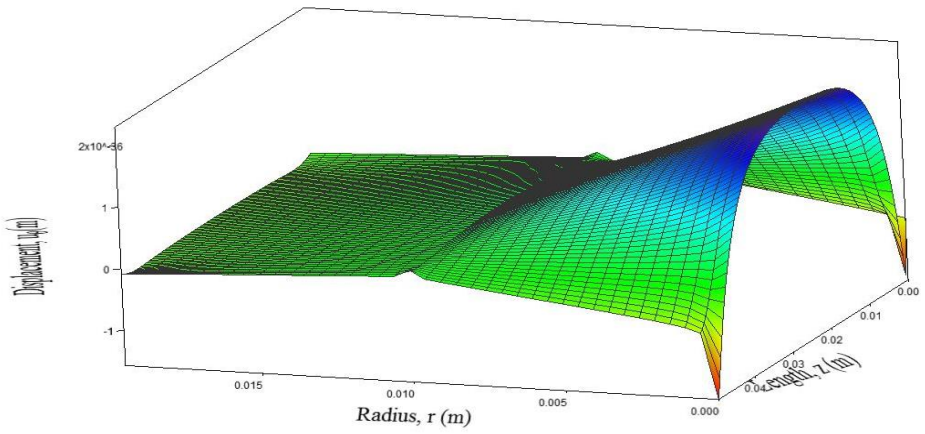

Fig. 33: Distribution of displacement components u_θ

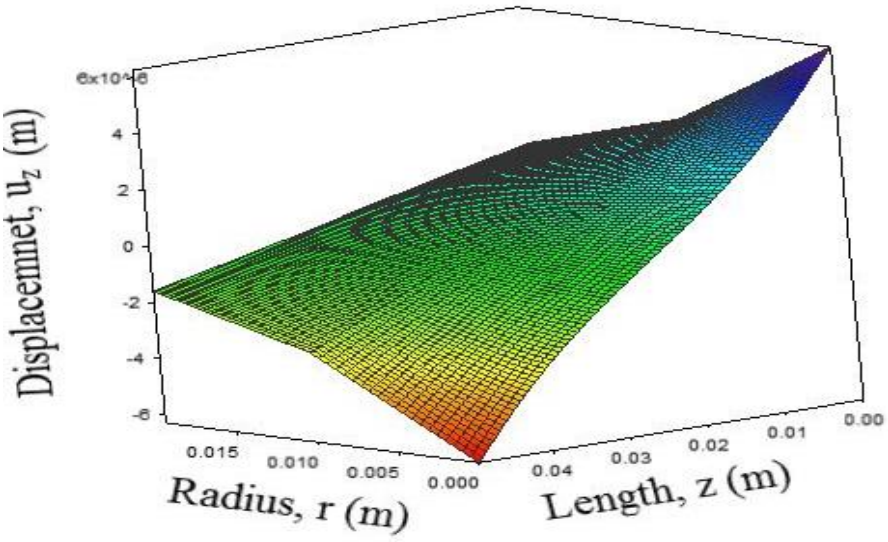

Fig. 34: Distribution of displacement components u_z

From figure 33 and 34 distribution of displacement components around the surface of the cylinder is plotted. For components change is constant for the outside cylinder and sharp change of displacement occurs for the inside cylinder. For components distribution is linear throughout the surface. Nature of the 2D curves and 3D surface plots are same.

CONCLUSION

In this work the displacement and stress distribution along radius subjected to internal and external pressure is investigated. Both 2D and 3D models are analyzed. Materials and the boundary conditions like pressure load and temperature are changed to observe the stress and displacement variation. Analytical solutions are presented. The results obtained in this analysis leads to the following conclusions:

a) The combined effects of temperature and pressure must be taken into account when designing compound cylinders, to ensure maximum efficiency and maximum availability.

b) The hoop stress is more effect by temperature then the internal pressure.

c) The value of stresses are higher in the interface region than the other places.

d) The normal stresses are always symmetric whereas shear stress show both symmetric and anti symmetric nature.

e) The internal pressure effect is more important when they are made from same materials than different materials.

REFERENCES

I. "Introduction to Composites", "http://nptel.ac.in/courses/112104168".

II. Choudhury Susanta, Roy H., Stress analysis of a thick walled cylinder. B Tech thesis, National Institute of Technology India, 2010.

III. F.C Campbell, "Introduction to Composite Materials".

IV. "Engineering constants", "nptel.ac.in/courses/101104010/lecture12/12_2.htm"

V. MdJakariaApu, Dr. Md Shahidul Islam, "Investigation of Displacement, Strain and Stress in Single Step Transversely Isotropic Elastic Bonded Joint".International Conference on Mechanical Engineering, ICME2015, BUET, Dhaka, Bangladesh, PP.0-46, 2015.

VI. Q. Zhang, Z. W. Wang, C. Y. Tang, D. P. Hu, P. Q. Liu and L. Z.

Xia, "Analytical solution of the thermo-mechanical stresses in a multilayered composite pressure vessel considering the influence of the closed ends", International Journal of Pressure Vessels and Piping, Vol. 98, PP.102-110, 2012.

VII. K. Vedeld, H. A. Sollund and J. Hellesland,"Closed analytical expressions for stress distributions in two-layer cylinders and their application to offshore lined and clad pipes", Journal of Offshore Mechanics and Arctic Engineering, Vol. 137, Isuue 2 PP.021702-021702-9, 2015.

VIII. H. A. Sollund, K. Vedeld and J. Hellesland, "Efficient analytical solution for heated and pressurized multi-layer cylinder Ocean Engineering", Vol.92, PP.285-295, 2014.

IX. E. David, "An overview of advanced materials for hydrogen storage", Journal of Material Processing Technology, Vol.162–163 PP.169-177, 2005.

X. W. R. D. Wilson and W. J. Skelton, "Design of bi-metallic high pressure cylinders", Proc. Inst. Mech. Eng., Vol.3, PP.1-10, 1967.

XI. A. H. Ghosn and M. Sabbaghian, "Quasi-static coupled problems of thermoelasticity for cylindrical regions", Journal of Thermal Stresses, Vol.5, PP.299-313, 1982.

XII. C. I. Hung, C. K. Chen and Z. Y. Lee, "Thermoelastic transient response of multilayered hollow cylinder with initial interface pressure", Journal of Thermal Stresses, Vol.24, PP.987-1006, 2001.

XIII. Z. Y. Lee, "Generalized coupled transient thermoelastic problem of multilayered hollow cylinder with hybrid boundary conditions", International Communications in Heat and Mass Transfer, Vol.33, PP.518-528, 2006.

XIV. S. Xu & M. Yu, "Shakedown Analysis of thick walled cylinders subjected to internal pressure with inified strength criterion", International Journal of Pressure vessels & piping, Vol. 82, PP.706-712, 2005

XV. M. Imaninejad & G. Subhash, "Proportional loading of thick walled cylinders", International Journal of Pressure vessels & piping, Vol. 82, PP.129-135, 2005.

XVI. P. Poworoznek., "Elastic-Plastic Behavior of a Cylinder Subject to Mechanical and Thermal Loads", Master's Thesis, 2008.